J. Fluid Mech. (1989), *vol.* 204, *pp.* 229–244
Printed in Great Britain

Reverse flow in a channel with an obstruction at the entry

By B. H. LAKSHMANA GOWDA[1] AND E. G. TULAPURKARA[2]

[1] Fluid Mechanics Laboratory, Department of Applied Mechanics, Indian Institute of Technology, Madras-600036, India

[2] Department of Aeronautical Engineering, Indian Institute of Technology, Madras-600036, India

(Received 23 May 1988 and in revised form 23 January 1989)

In this study the flow through and around a parallel-walled channel with an obstruction (flat plate) placed at the channel inlet is investigated. Depending on the position of the obstruction, the flow inside the channel is in a direction opposite to that outside, stagnant or in the same direction as outside but with reduced magnitude. Flow visualization in water is used to examine the fluid motion, although some wind tunnel measurements have been made and are also reported. The parameters that have been varied are the gap between the obstruction and the entry to the channel, the length of the channel and the Reynolds number. The maximum value of the reverse flow velocity is found to be about 20% of that of the flow outside. The maximum forward velocity inside the channel (when it occurs) is only about 65% of the outside velocity even for very large gaps between the obstruction and the channel entrance. A tentative explanation is offered for the observed features.

1. Introduction

The present investigation is an off-shoot of the attempts of the authors to obtain very low velocities by controlling the entry flow in a channel placed within another wider channel. The configuration is schematically shown in figure 1, where the inner channel is referred to as the test channel. For certain positions of the flow control device, a flat plate near the entry to the test channel, it is found that the flow in the test channel is almost stagnant and sometimes is in a direction opposite to that of the outside flow. The latter phenomenon prompted the authors to investigate the flow in more detail. Some of the parameters that affect the flow are the gap between the test channel and flow control device (g), the length of the test channel (L) and the Reynolds number (Re) based on the channel width (w) and velocity outside the channel (U_0). These parameters have been systematically varied and their influence on the flow in general and the velocity inside the test channel (U_i) in particular is investigated. Some of the possibilities where the flow phenomenon that has been observed and described in this paper can occur or can be employed are: control of flow, especially to obtain low velocities; heat transfer problems where it may be required to locally have different types of flows; interaction of shear layers at varying distances apart; flow past obstructions/constrictions in arterial flows under certain physiological situations.

There appears to be no direct reference in the literature to the problem reported here though there is a large body of information concerning flow control using different types of valves (Streeter 1961; Davis & Sorenson 1969; Hutchison 1976;

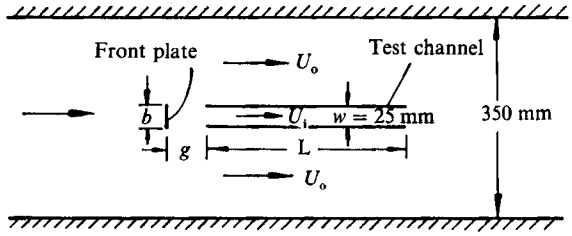

FIGURE 1. The test arrangement.

Eom 1988). Also there are studies dealing with the mechanism of vortex formation and shedding (Gerrard 1966) and the interaction of two shear layers with different spacing in between (Abernathy & Kronauer 1962). Unal & Rockwell (1988*a*,*b*) have described the vortex shedding process from a circular cylinder and the influence of a splitter plate behind in the Reynolds-number range 140–5000. These results have some relevance to the present investigation and are referred to at a later stage. The above studies, however, appear not to have a direct bearing on this problem.

The investigation deals mainly with flow visualization results at low Reynolds numbers. Some experiments have been carried out at a higher Reynolds number using a different set-up, mainly to see whether the observed phenomena at low Reynolds numbers occurs at the higher value also.

2. Flow visualization study

2.1 *Experimental set-up*

The experiments are carried out in a recirculating water channel. The arrangement is essentially the same as that used by the authors in an earlier investigation (Tulapurkara, Lakshmana Gowda & Balachandran 1988) and is shown schematically in figure 2. It consists of a tank 2.5 × 1.5 m with a depth of 150 mm, at one end of which are located two sets of aluminium discs (vanes) with suitable spacing in between them. When these vanes are rotated they act as paddles and create a flow which is suitably guided to the test section where the model is placed. A variable speed d.c. motor is used for rotating the vanes and a fairly wide range of flow speeds can be achieved in the test section. The fluid in the tank is water and fine aluminium powder is used as tracer medium. Photographs are taken by mounting the camera at a suitable location above the model. Proper lighting is obtained by using halogen lamps.

The experimental set-up is shown in figure 1. The width of the test channel w and also the width of the obstruction plate b are equal to 25 mm. To study the effect of gap width, g, it is varied from 12.5 to 200 m, giving a g/w ratio between 0.5 and 8. This investigation is done for two values of test channel length L, viz. 600 and 300 mm (L/w = 24 and 12). Results are obtained at the Reynolds numbers (based on the velocity U_0 and the width w) 2000, 3000 and 4000. The effect of the length of the channel L on the flow phenomenon is studied at $g/w = 1$ and $Re = 4000$ for L equal to 105, 210, 300, 400, 500 and 600 mm (L/w = 4.2, 8.4, 12, 16, 20 and 24). The influence of Re is studied with $g/w = 1$ and two values of L/w equal to 24 and 12. Flow past the plate alone is also studied at various Reynolds numbers.

An SLR Pentax camera with a normal lens and a wide angle lens is used to photograph the flow field. The wide angle lens is necessary at the higher L/w ratios. The camera speed is $\frac{1}{8}$ s except in figure 9(*a*,*b*) where it is $\frac{1}{4}$ s. The most important

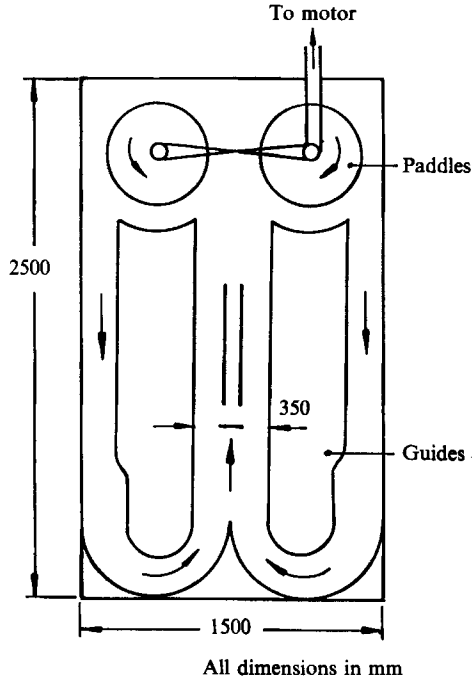

FIGURE 2. Schematic view of the flow visualization tank.

features of the flow are found to occur in the regions near the entry and exit of the test channel. To capture these flow details in photographs of manageable length, only negatives showing the entry and exit are printed. Since the central part of the test channel is not included in the negatives, the photographs in figures 3, 4 and 6–9 are pasted side-by-side with a small gap. The gap is present to indicate that the flow pattern shown in the right half of the figure does not occur immediately downstream of the flow shown in the left half. In each figure care has been taken to retain the essential portions of the flow at both ends of the test channel.

Details of the measurements carried out in a wind tunnel are described in § 3.

2.2 *Results and discussion*

2.2.1. *Effect of gap g*

This study is carried out for $L = 600$ and 300 mm. For each value of L, results are obtained at $g/w = 0.5$, 1, 1.5, 2, 2.5, 3, 3.5, 4, 4.5, 5, 5.5, 6, 7 and 8. Photographs at selected values of g/w are shown in figures 3 and 4.

Figure 3(*a*,*b*) clearly shows that the flow in the test channel is in a direction opposite to that of the flow outside. The value of U_i/U_o is -0.15 for $g/w = 0.5$; U_i is the velocity inside the test channel and U_o is the velocity in the free stream outside (figure 1). The velocity U_i is obtained from the time taken by a tracer particle to cover a fixed distance in the central part of the test channel. For $L = 600$ mm, this distance is 200 mm. In all cases U_i and U_o are measured several times (on an average four times) and the mean taken. As g/w is increased the magnitude of the reverse flow increases (i.e. U_i/U_o becomes more negative) until a maximum is reached for $g/w = 1.5$ (figures 3*b* and 5*a*). Beyond this value of g/w, the reverse flow weakens and at $g/w = 3.5$, the flow in the test channel is stagnant (figure 3*d*). With further increase in g/w there is at first a slow forward motion which strengthens as g/w

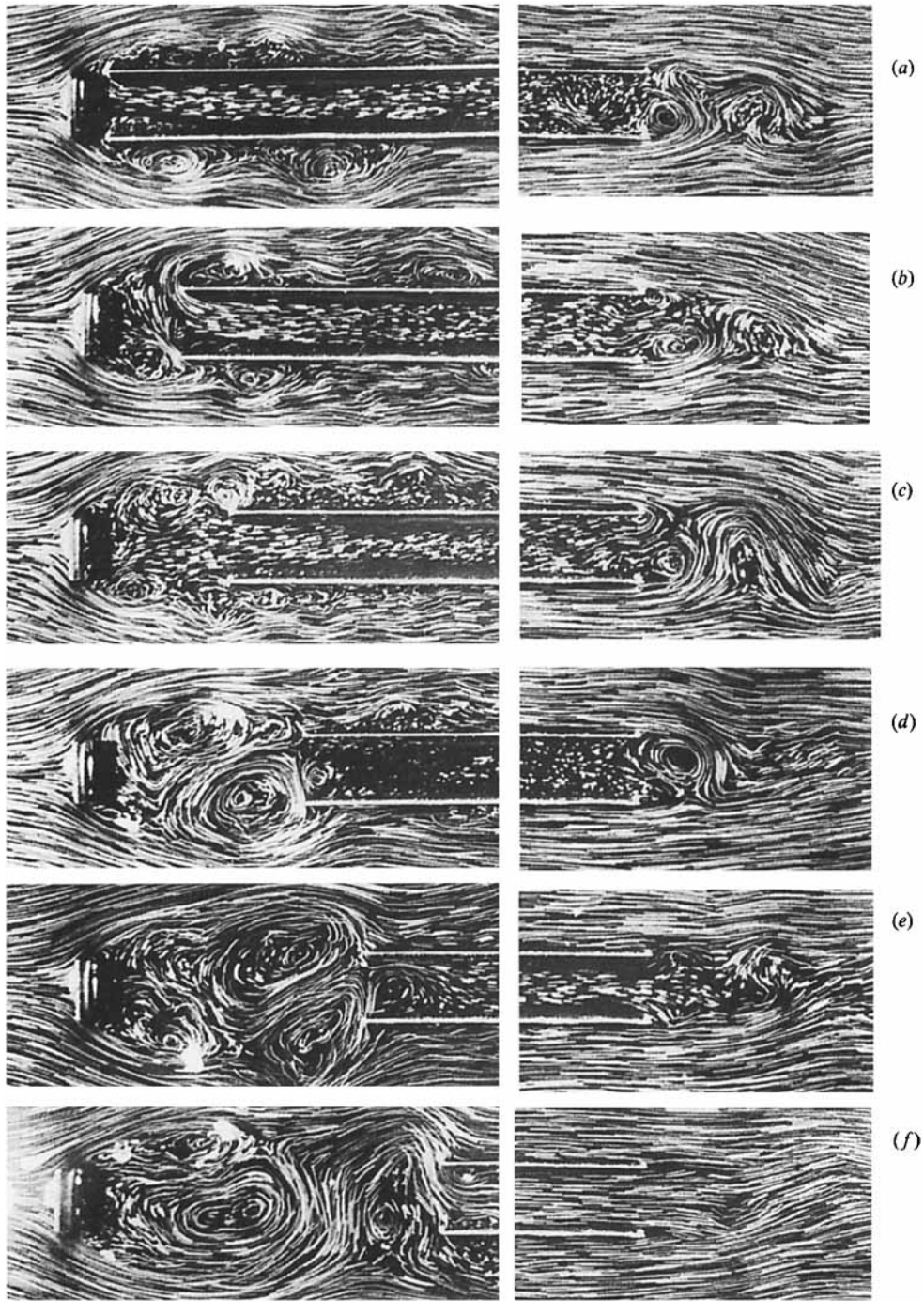

FIGURE 3. Effect of gap ($L = 600$, $Re = 4000$): (*a*) $g/w = 0.05$, (*b*) 1.5, (*c*) 2.5, (*d*) 3.5, (*e*) 4.5, (*f*) 6.0

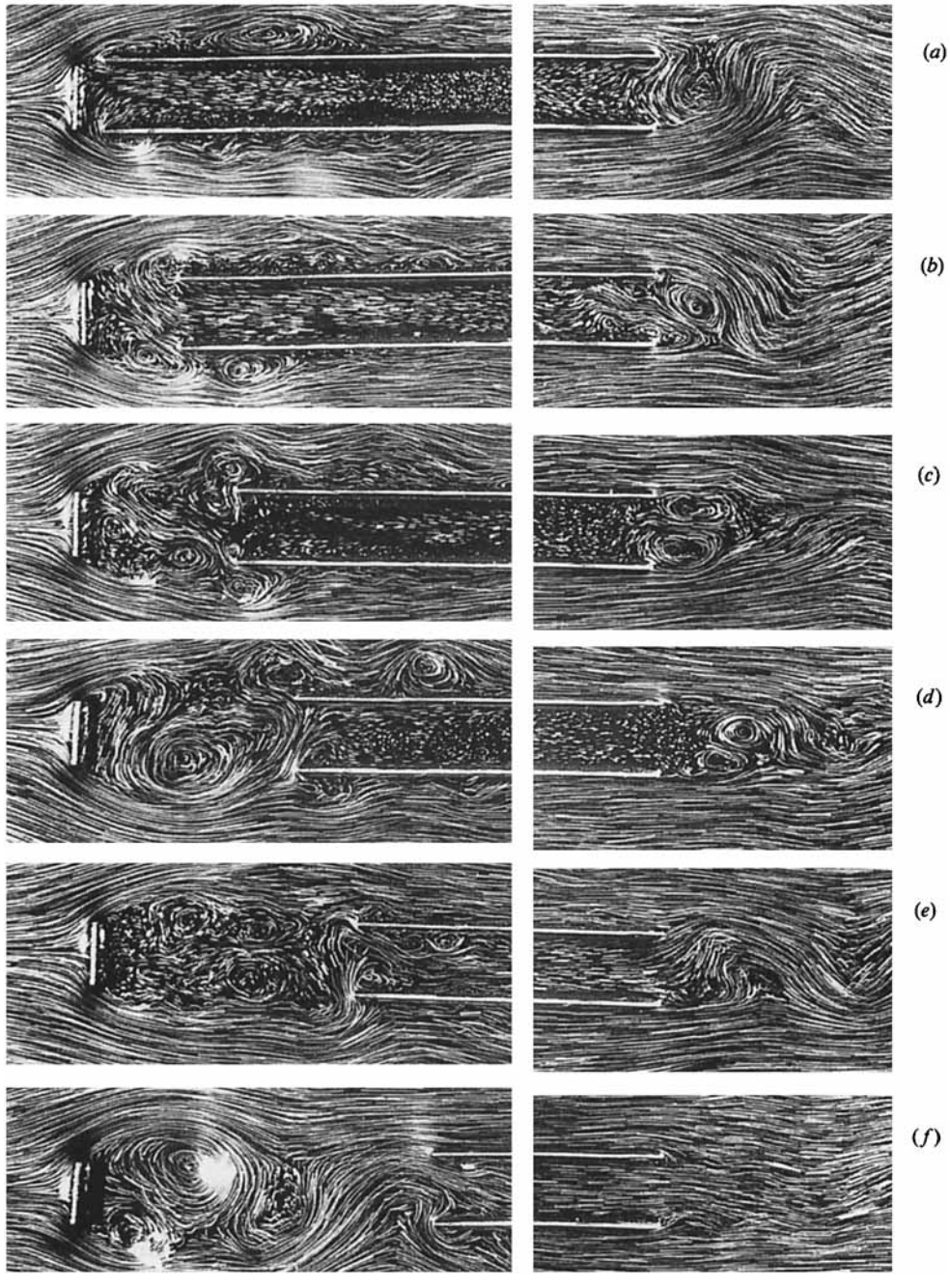

FIGURE 4. Effect of gap ($L = 300$, $Re = 4000$): (*a*) $g/w = 0.5$, (*b*) 1.5 (*c*) 2.5, (*d*) 3.5, (*e*) 4.0, (*f*) 6.0.

increases (figure 3*e*,*f*). But even for $g/w = 8$, the value of U_i/U_o is only 0.65 (figure 5*a*). The photographs of the flow when L is 300 mm are shown in figure 4, and are seen to be similar to the $L = 600$ mm case. The variation of U_i/U_o with g/w is included in figure 5(*a*). The values of U_i/U_o for $L/w = 8.4$ and $Re = 4000$ at $g/w = 1$, 4 and 6 shown in the figure compare reasonably well with the trend for $L/w = 12$ and 24 at $Re = 4000$.

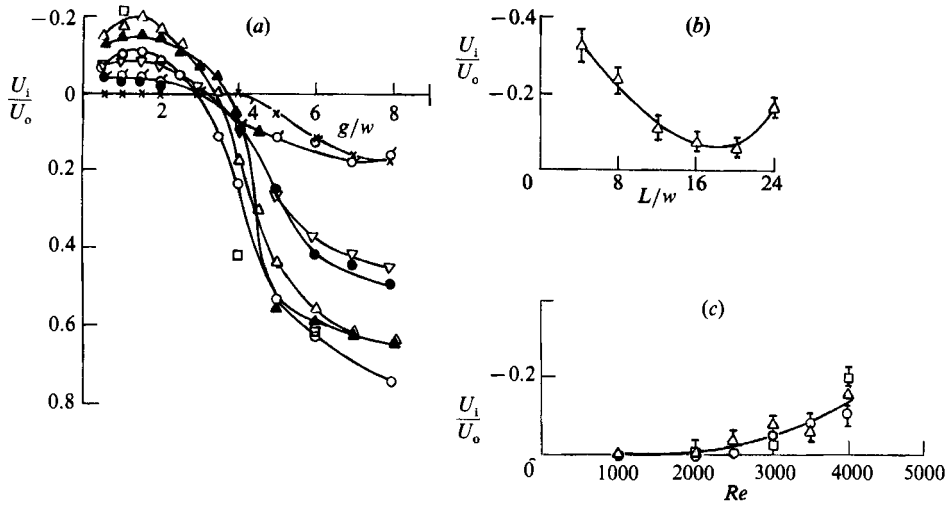

FIGURE 5. Influence of various parameters on U_i/U_o. (*a*) Gap effect △, $L/w = 24$, $Re = 4000$; ○, $L/w = 12$, $Re = 4000$; □, $L/w = 8.4$, $Re = 4000$; ▲, $L/w = 24$, $Re = 2.6 \times 10^4$; ●, $L/w = 12$, $Re = 3000$; ▽, $L/w = 24$, $Re = 3000$; ×, $L/w = 12$, $Re = 2000$; ♂, $L/w = 24$, $Re = 2000$. (*b*) Length effect at $g/w = 1$, $Re = 4000$. (*c*) Effects of Re at $g/w = 1$: △, $L/w = 24$; ○, $L/w = 12$; □, $L/w = 8.4$.

In figure 5(*a*) the results at $Re = 2000$ and 3000 for $L/w = 12$ and 24 are also included. For $L/w = 12$ and at $Re = 2000$, the flow inside the test channel is stagnant until $g/w = 4$, beyond which there is weak forward flow. But for $L/w = 24$, at the same Re there is reverse flow at lower values of g/w, though its value is small ($U_i/U_o \approx -0.05$). At $Re = 3000$, the reverse flow occurs both for $L/w = 12$ and 24, but it is stronger for the longer plate. This feature (i.e. a stonger reverse flow for $L/w = 24$ than for $L/w = 12$) is observed at $Re = 4000$ also and is further discussed in §2.2.3.

It should be added that the flow near the entry and exit of the test channel is unsteady. The vortex shedding near the entry and/or exit causes the flow to enter or leave the test channel from its left half or right half (figures 3*b*, 6*a*, 6*d*). Sometimes it may leave in a symmetric manner (figures 3*a*, 6*c*). However, the flow in the central portion of the test channel, away from the entry and exit, has fairly steady average velocity.

A tentative explanation for the observed features is given in §2.2.4 after the results for flow around flat plate have been presented.

2.2.2. *Influence of length L*

The influence of the length of the test channel on the magnitude of the velocity ratio U_i/U_o is investiaged for $g/w = 1$ and $Re = 4000$. Results are obtained for $L = 105$, 210, 300, 400, 500 and 600 mm, i.e. $L/w = 4.2$, 8.4, 12, 16, 20 and 24, and photographs are shown in figure 6. For $L/w = 4.2$ (figure 6*a*), the shear layers separating from the front flat plate extend almost to the end of the test channel and a strong recirculating flow is seen. The value of U_i/U_o is plotted in figure 5(*b*). For lengths smaller than 105 mm, U_i could not be measured with confidence. As the length of the test channel increases, U_i/U_o decreases and a minimum is reached for $L = 500$ mm. For $L = 600$ mm U_i/U_o shows a considerable increase, as shown in figure 5(*b*).

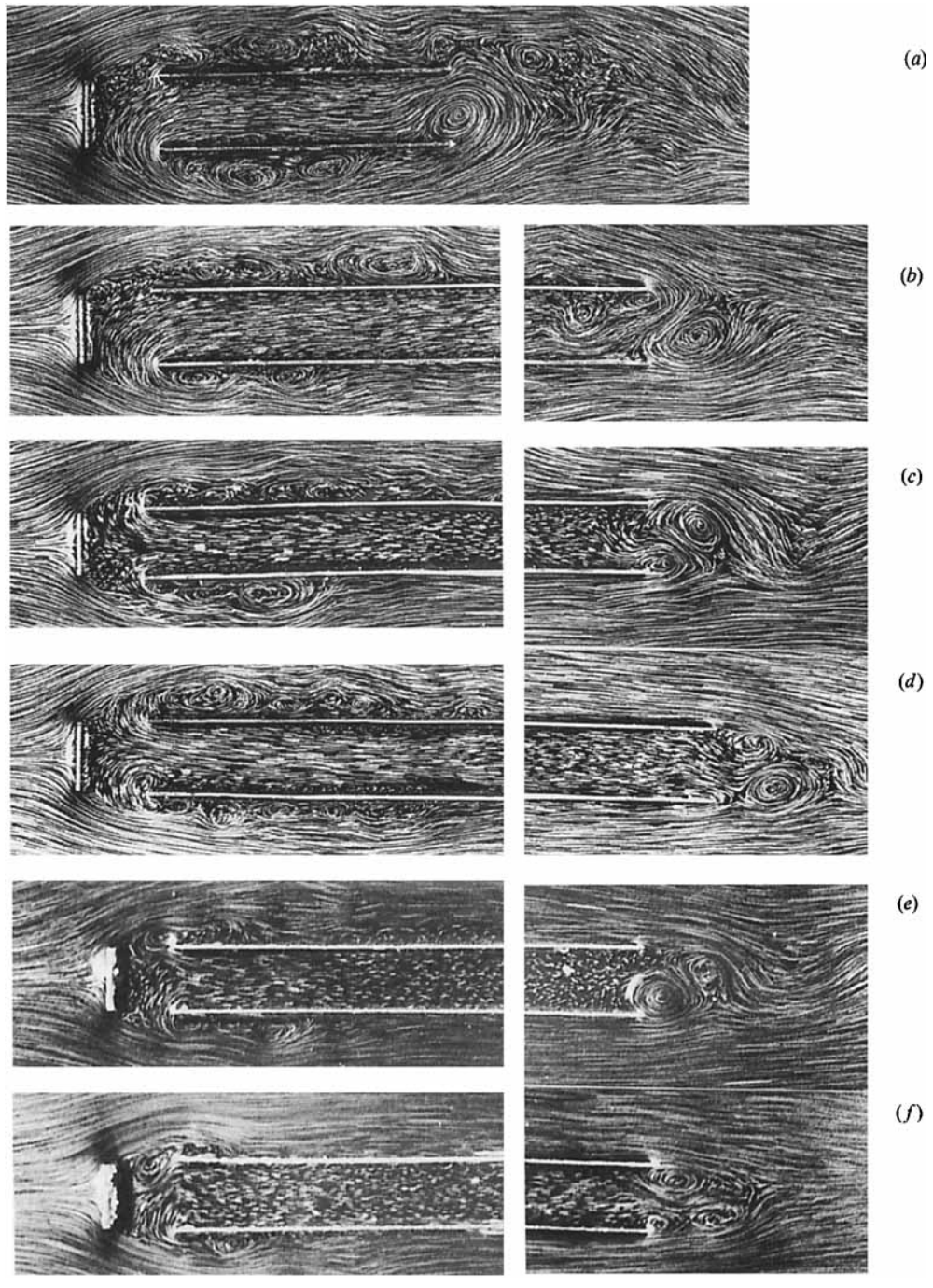

FIGURE 6. Effect of channel length ($Re = 4000$, $g/w = 1$): (*a*) $L/w = 4.2$, (*b*) 8.4, (*c*) 12, (*d*) 16, (*e*) 20, (*f*) 24.

If it is assumed that the flow in the reverse direction is caused by the low base pressure behind the front flat plate, then it is expected that the velocity in the reverse direction would decrease as the length of the test channel increases. But it is not clear why it increases for $L/w = 24$ after having a minimum for L/w around 20. However,

the flow pattern at the rear does offer some explanation (figure 6*e*,*f*). In the case of $L/w = 20$, the vortices formed at the rear end are found to be larger and remain longer near the exit and there is effectively less pumping in of fluid. Whereas, at $L/w = 24$ the vortices are smaller and are shed rapidly (figure 6*f*). The flow pattern is such as to create good inflow into the test channel. Of course it would be very interesting to see what happens when L is further increased. It has not been possible to increase L beyond 600 mm owing to experimental set-up limitations.

2.2.3. *Influence of Reynolds number*

The influence of Reynolds number is studied for $L = 600$ and 300 mm at $g/w = 1$. The results are shown in figures 7 and 8.

Almost stagnant conditions prevail in the test channel up to $Re = 2000$. The shear layers at the rear end of the test channel form a wedge-like region; but there is no vortex shedding (figure 7*a*). As the Reynolds number increases the two shear layers at this end interact and vortex shedding begins and gives rise to flow in the reverse direction (figure 7*b*–*f*). In both cases, i.e. $L = 600$ and 300 mm, the value of U_i/U_0 increase with Re (figure 5*c*). It was remarked in §2.2.1 that at $Re = 3000$ and 4000 U_i/U_0 is more negative for $L = 600$ mm than for $L = 300$ mm. This is a bit surprising as one would expect a stronger mutual interaction between the low base pressure at the front end (created because of the flat plate) and the flow at the rear end for shorter lengths, which should lead to larger values of U_i/U_0. It may be surmised that Reynolds number has a complex influence on the vortex shedding at the rear end of the channel. The pumping-in that occurs at the rear end, though influenced by the low pressures at the front end, may have an independent role in generating the high values of U_i/U_0 observed at $L = 600$ mm. The mechanism of generation of vortical flows at the rear end and energy dissipated for various lengths of the test channel needs to be looked into in detail. The relative thickness of the shear layers that are formed at the rear end might be playing an important role. Quantitative measurements of these are required to further understand the observed features.

2.2.4. *Flow around the front flat plate*

To obtain further insight the flow past the front flat plate alone is studied at Reynolds numbers from 650 to 4000. Several aspects of flow past a flat plate have been studied (e.g. Kiya & Matsumara 1988; Gerrard 1978, Perry & Steiner 1987) but visualization studies of flow past a plate are very limited. Batchelor (1967) has reproduced the aluminium particle flow visualizations of Prandtl and Tietjens, but the maximum Reynolds number is only 250. Chang (1970) has presented photographs of smoke flow past a plate at Re between 820 and 7350. The aim of the photographs is to indicate the surface of discontinuity starting from the edge of the plate. Details of the flow behind the plate are not clear. Pierce (1961) has presented photographs of vortex shedding from the edges of a plate accelerated normal to itself from rest in still air. A spark-lighted shadograph technique has been used to study the development of the vortex sheet roll-up. Recently Smits (1982) has obtained instantaneous pictures of flow past a flat plate using smoke at $Re = 3400$.

However, these studies do not give the information needed in the present study and hence flow patterns have been obtained for $Re = 650$ to 4000. In this case the Reynolds number is based on the free-stream velocity and the plate width. Photographs at selected Reynolds numbers are presented in figure 9. Though the results for Re below 2000 are not directly relevant, they are included for completeness.

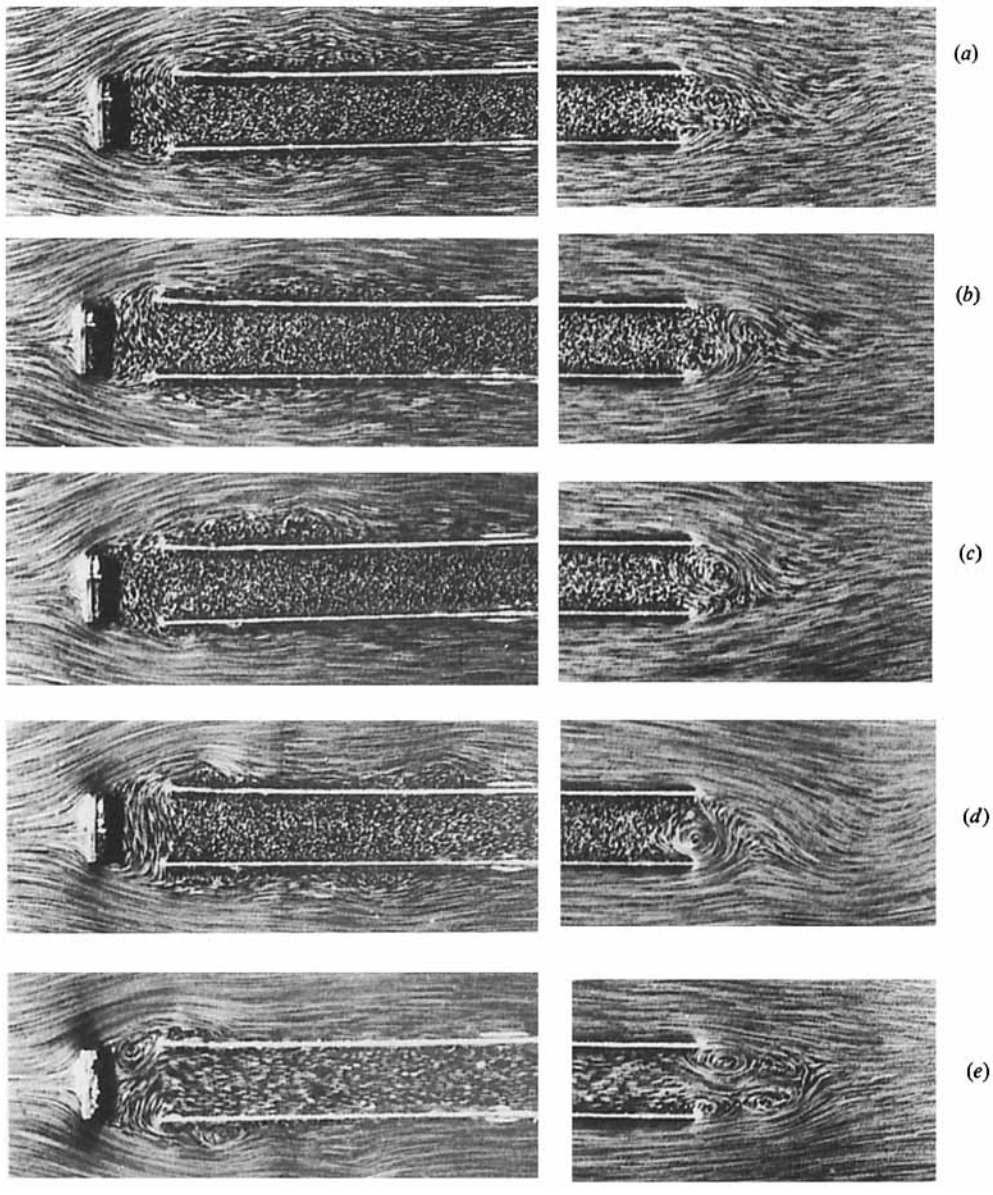

FIGURE 7. Influence of Reynolds number ($L = 600$, $g/w = 1$): (*a*) $Re = 2000$, (*b*) 2500, (*c*) 3000, (*d*) 3550, (*e*) 4050.

At low values of Re the rolling up process is slower and vortices are formed at some distance behind the plate (figure 9*a*,*b*). As Re increases the rolling up is faster and the vortices are formed closer to the plate (figure 9*c*–*e*). At $Re = 4000$ the vortex is formed just behind with the core located at about one width away from the plate (9*f*). The camera speed is $\frac{1}{4}$ s in figure 9(*a*,*b*) and $\frac{1}{8}$ s in figure 9(*c*–*f*). This is done to show the rolling up process more clearly at low Reynolds numbers.

When the test channel is placed behind the plate, the flow behind the latter is considerably altered and depends on the distance between the test channel and the plate (figures 3*a*–*f* and 9*f*). Also at any given value of g/w it will depend on Re (figures

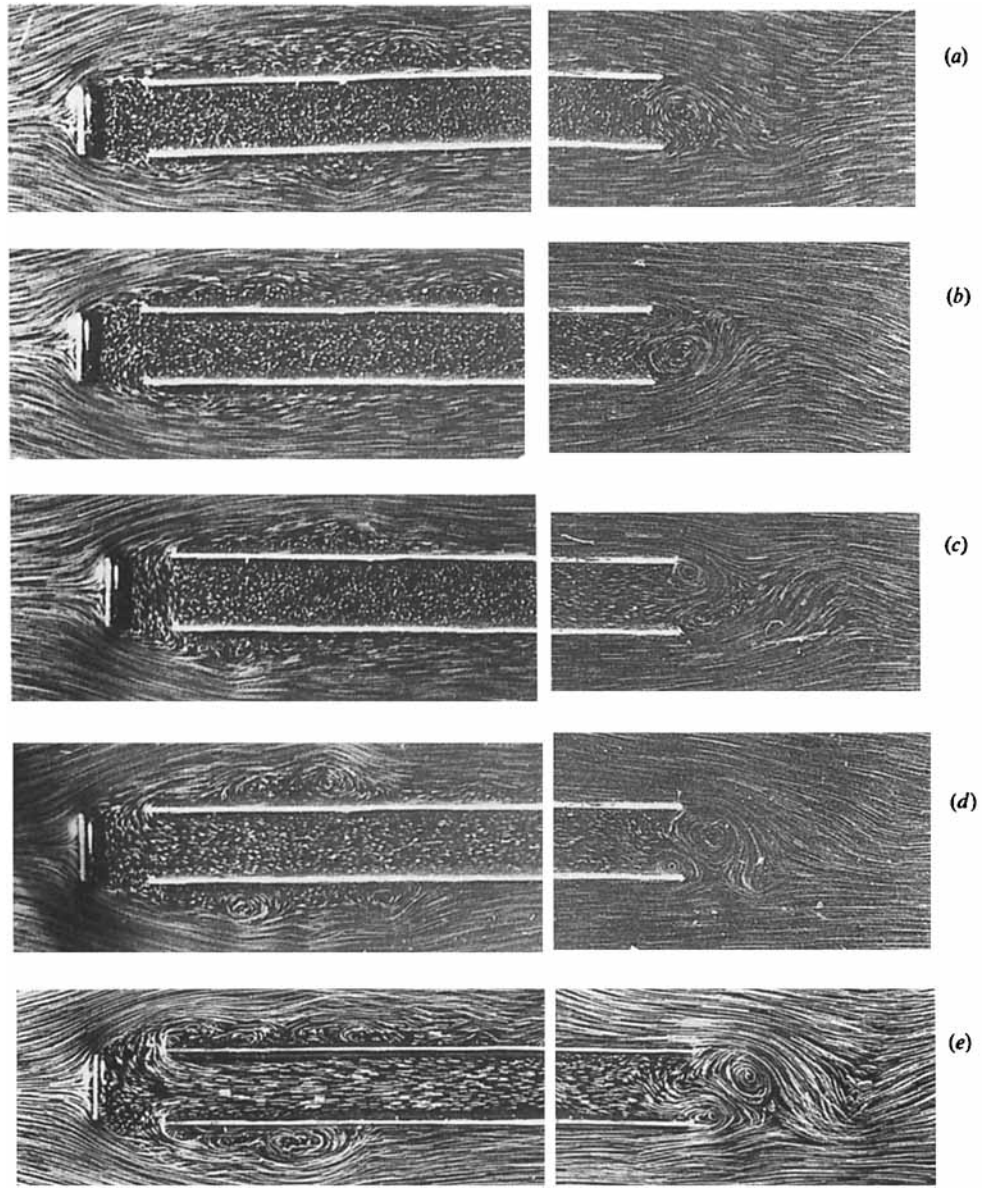

FIGURE 8. Influence of Reynolds number ($L = 300$, $g/w = 1$): (*a*) $Re = 2000$, (*b*) 2500, (*c*) 3000, (*d*) 3500, (*e*) 4000.

7*a*,*c*,*e*, 9*d*,*e*,*f*). Let us first consider the effect of gap. Comparison of figures 9(*f*) and 3(*a*–*f*) shows that when the gap is small, say $g/w = 0.5$ or 1, the shear layers starting from the edges of the front plate reattach to the sidewalls of the test channel. A region of low pressure exists behind the front plate and this triggers the reverse flow in the test channel. Consequently at the rear end of the channel the fluid streams meet at different velocities and when the Reynolds number is not too low (say more than 2000) the shear layers, starting from the rear ends of both sides of the test channel, become unstable and this leads to alternate vortex shedding at the rear end of the test channel (figure 7*b*) and 'pumping' of the fluid starts. Subsequently when the

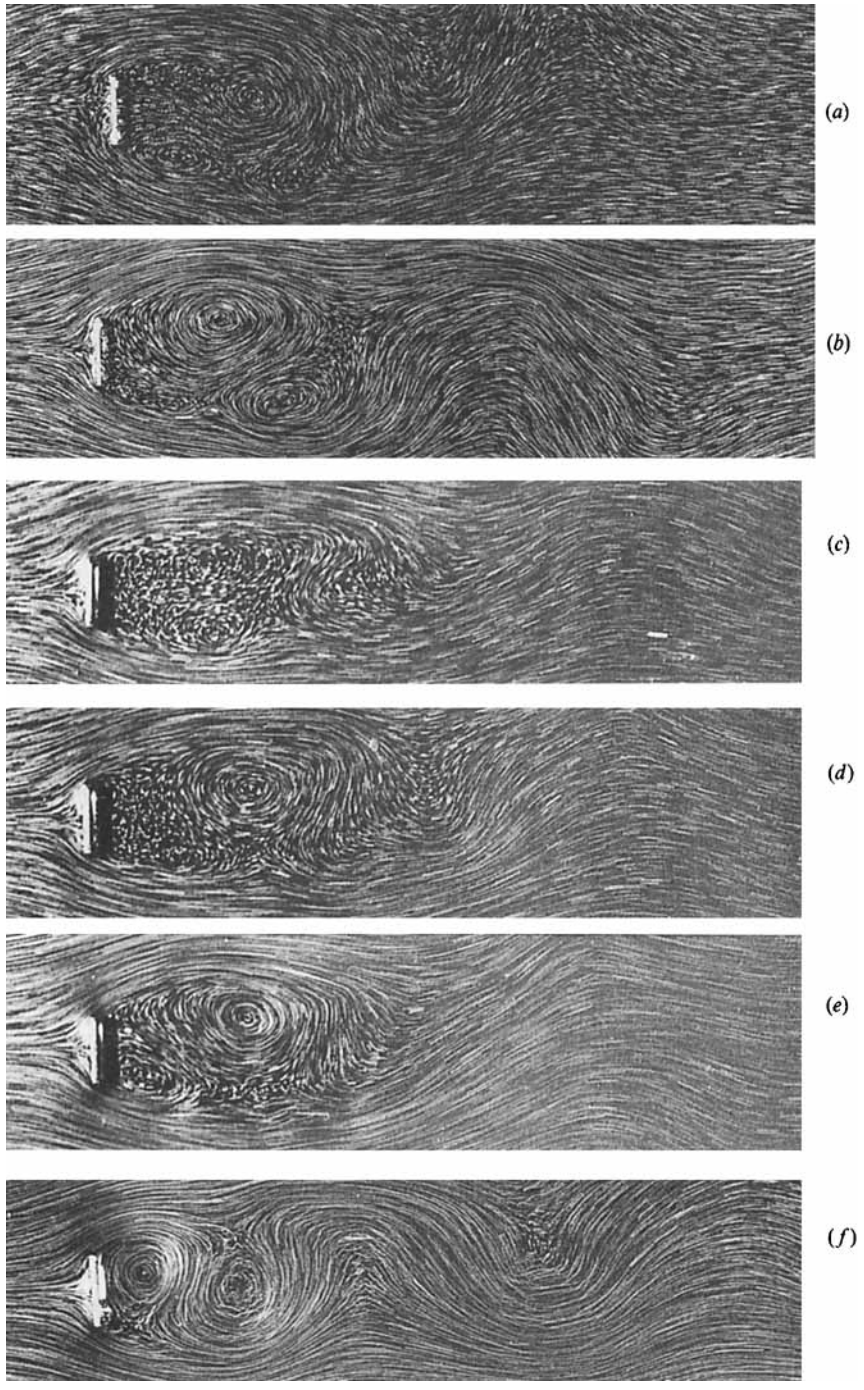

FIGURE 9. Flow past plate at various Reynolds numbers: (*a*) $Re = 670$, (*b*) 1050, (*c*) 1500, (*d*) 2000, (*e*) 3000, (*f*) 4000. The camera speed for (*a*), (*b*) is $\frac{1}{4}$ s, rather than the $\frac{1}{8}$ s used in (*c–f*) and the other figures.

flow has established itself the points of reattachment of shear layers from the front plate and the vortex shedding at the rear end vary in a periodic manner but there is, on average, continuous reverse flow in the central part of the test channel. The velocity of reverse flow would depend on the static pressure at the entry to the test channel, the losses in the test channel as well as the energy dissipated in the vortex sheddding at the rear end of test channel.

As the gap between the front plate and the test channel increases the mutual interference between the two decreases. The shear layers starting from edges of the front plate can now roll up in the gap between the front plate and the test channel. The pressure at the entry to the test channel is not so low and the reverse flow weakens and stops for some g/w. The flow field between the plate and channel also contribute to this, with the vortices behind the plate having a sort of 'sealing' effect (figures 3*d* and 4*d*). The vortex shedding at the rear end of the channel, however, continues because the fluid streams still have widely different velocities at the exit (figure 3*d*). At still higher values of g/w (> 3.5) the vortices formed behind the flat plate 'pump' in fluid in the forward direction as in figures 3(*e*,*f*) and 4(*e*,*f*). With further increase in the gap the vortices shed from the plate even have time to decay before they reach the test channel. Owing to the pressure losses occurring, the forward velocity in the test channel does not reach the value outside it even when the gap is quite large.

It may be relevant here to compare the interference effects of the test channel on the vortex shedding process behind the flat plate with the results of Unal & Rockwell (1988 *a*,*b*). Their investigations deal with the interference effects of a splitter plate on the vortex formation and shedding from a circular cylinder. The splitter plate is placed behind the cylinder, along the centreline of the wake at various distances, i.e. the gap between the cylinder base and leading edge of the plate is varied. One observation is that, at sufficiently low Reynolds numbers, the von Kármán regime of the corresponding free wake can be completely suppressed when the plate is placed sufficiently close to the cylinder. When the plate is located downstream of one or more fully formed vortices, the formation length of the first vortex changes. In general, the interaction between the near wake and splitter plate are found to change with the Reynolds number in the range considered.

It is quite interesting to note similar effects in this study though the problems considered are much different. In comparison to the study of Unal & Rockwell, the sides of the test channel here interfere with the shear layers from the front plate at some distance away from the centre line of the wake of the plate. Owing to this the vortex formation and shedding process is disrupted up to $g/w = 2.5$ at $Re = 4000$ (figure 3a,*b*,*c*). Only at $g/w = 3.5$ can the vortex formation be seen (figure 3*d*); but the vortex formation length is different from that for the free wake of the plate (figure 9*f*). At still larger g/w (figure 3*f*) the change in the formation length of the first vortex is clear to see, as also is the distortion of the vortices compared to that in figure 9(*f*). Even at a g/w value of 8 the test channel is seen to considerably influence the flow behind the plate. Of course it is also this process which contributes considerably to the determination of the volumetric flow through the test channel.

Considering the influence of Re at a particular value of g/w ($= 1$), figure 7(*a*,*c*,*e*) and figure 9(*d*,*e*,*f*) taken together show some interesting factors and also reveal the reasons for the trends observed in figure 5(*a*) for $Re = 2000$, 3000 and 4000. At $Re = 2000$ (figures 9*d* and 7*a*) the distance between the plate and the test channel is less than the formations length of the vortices (figure 9*d*) and the separated shear layers from the plate attach on to the sides of the test channel at sufficiently larger

downstream distances (figure 7*a*). The situation changes as Re increases (compare figures 9*e*, 7*c* to 9*f*, 7*e*). It is seen that the vortices are formed just behind the plate at $Re = 4000$ (figure 9*f*) and one can expect no further change in the formation length for $Re > 4000$. This means that the magnitudes and the trend in the variation of U_i/U_0 can be expected to remain the same beyond $Re = 4000$. Interestingly, this has been shown to be the case as the results at higher Re conducted in a wind tunnel facility have shown. These will be presented below.

From the above explanation and the experimental observations it can be concluded that a Reynolds number of 2000 or above is needed for the start of the reverse flow and that a gap of 1.5 times the channel width gives maximum reverse flow. But the role of the length of the channel seems to be more complicated and needs further investigation.

3. Wind tunnel experiments

To examine whether the features observed at rather low Reynolds numbers (in the flow visualization experiments) occur at a higher Reynolds number, some measurements have been made using a wind tunnel facility. The test arrangement is schematically shown in figure 10(*a*, *b*). Air is supplied from a centrifugal blower and it is controlled by a throttle placed in the inlet section. The air stream is led into a settling chamber (through a set of four screens) which terminates in a smooth nozzle section made out of fine teak wood with a exit cross-section of 130×245 mm. The velocity at the exit is checked before fixing the test section, both in the horizontal and vertical planes passing through the centre of the nozzle. The velocity is very uniform, the variation being less than 0.5%.

The test section with a rectangular cross-section of 130×245 mm (to match the exit of the wind tunnel nozzle exit) and 1.8 m long is prepared out of 12 mm thick Plexiglas sheet. The two plates forming the test channel are made out of galvanised iron sheets, 1.5 mm in thickness and 600 mm in length are fixed within the test section (figure 10*b*). Aluminium angles ($10 \times 10 \times 3$ mm) with countersunk screws are used to fix the plates in the test section. Care is taken to check that the width between the plates throughout their length is equal to 25 mm (i.e. $w = 25$ mm). Another plate 1.5 mm thick and 130×25 mm in size is fixed at various distances near the front end of the inner channel. The relevant dimensions are shown in figure 10(*b*). At the largest value of the gap ratio ($g/w = 8$) the distance from the exit of the nozzle to the plate is 150 mm, i.e. six times the width of the plate. Provision is made to measure the velocity (U_i) at the central section of the test channel and also to measure the velocity (U_0) outside. This is done using Pitot and static probes made out of steel tubes with 1 mm outer diameter and 0.1 mm wall thickness conforming to standard design. A Furnace Controls (U.K.) digital micromanometer Type FC 012 with a least count of 0.01 mm is used to measure the Pitot and static pressures. All the measurements are carried out at a velocity U_0 equal to 15 m/s which corresponds to a Reynolds number of 2.6×10^4 referred to the velocity U_0 and width w of the test channel.

The magnitudes of both U_0 and U_i are obtained by fixing the front plate at different distances near the front end of the test channel, varying the g/w ratio from 0.5 to 8. At each position of plate the direction of U_i is checked by using a tuft held in the test section and also smoke from a incense stick. The reverse flow that occurs is clearly visible.

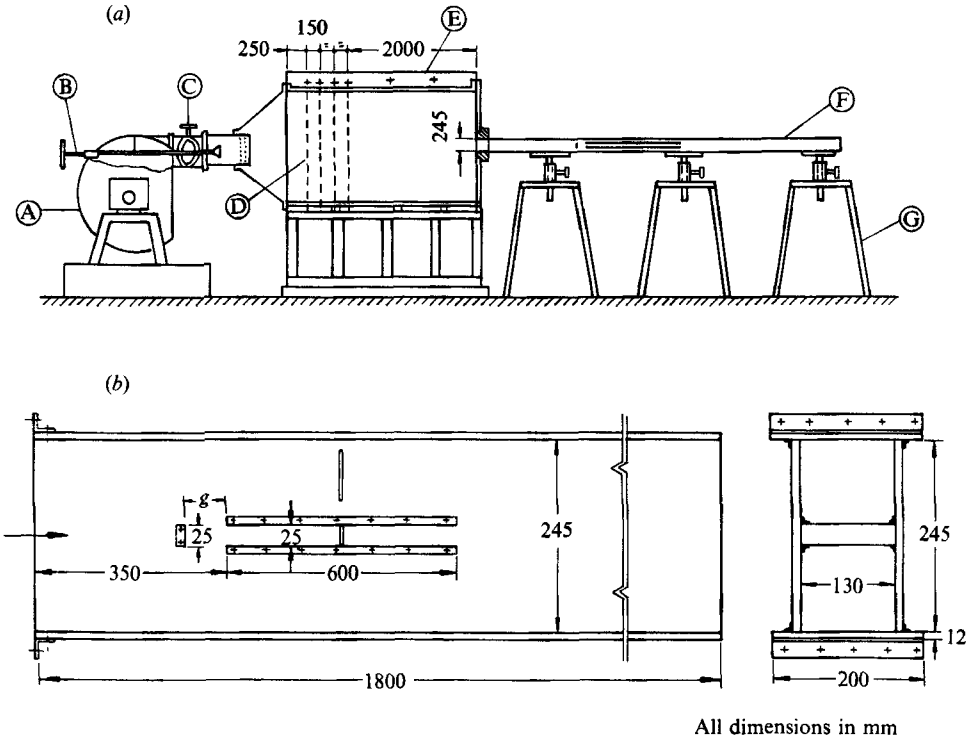

FIGURE 10. Test set-up for air experiments. (*a*) Wind tunnel set-up (all dimensions in mm). (A, Blower; B, Throttle control; C, Bypass control; D, Screens (40 mesh); E, Settling chamber (1000 × 1000); F, Test Section; G, Stand. (*b*) Test section details.

Figure 11 illustrates this for $g/w = 1.5$. Two tufts were introduced through holes at a station located at the midpoint of the test channel – one tuft inside the test channel and the other in the stream outside it. The main flow is from left to right as indicated by the upper tuft. The flow direction in the test channel is shown by the lower tuft. The velocity in the test channel is low and hence the lower tuft is not as straight as that in the flow outside.

The velocity ratio U_1/U_0 from wind tunnel tests is plotted in figure 5(*a*) along with the results obtained in the flow visualization study. The close agreement between the two clearly shows that the observed phenomenon is not restricted to low Reynolds numbers. Further, as mentioned in §2.2.4, the results indicate that the trend in the variation of U_1/U_0 may essentially remain same at Reynolds numbers greater than 4000.

4. Concluding remarks

There appear to be two main mechanisms that determine both the direction and magnitude of the flow in the configuration considered in this study: (*a*) the flow separation, subsequent reattachment and the low pressures created at the front end of the channel; (*b*) the generation of vortical flows due to the interaction of shear layers at the rear end of the channel. Both factors are dependent on g/w, L/w, b/w and Re, and on each other. The exact mechanism of interaction is not yet clear. Further quantitative measurements such as the magnitude of base pressures at the

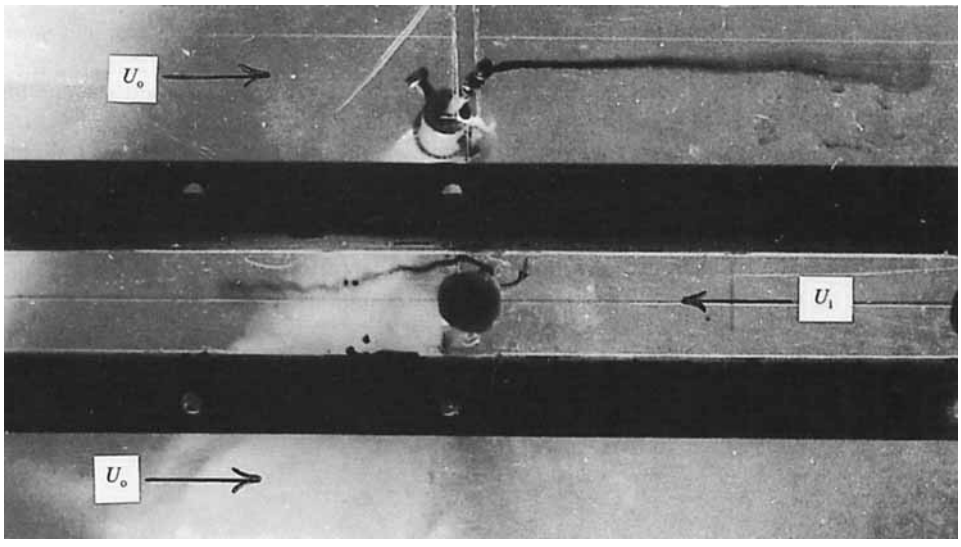

FIGURE 11. Visualization with tufts in wind tunnel experiments ($Re = 2.6 \times 10^4$).

front end, the pressure distribution along the channels, the shear layer thicknesses at the rear end etc. are required. In spite of the limited scope of the present study, the results reveal some very interesting features.

The following conclusions of a quantitive nature can be drawn from the results presented:

(*a*) For the case when the inner channel has a length of 24 times its width and the gap equal to the channel width, the flow in the reverse direction begins when Reynolds number is around 2000.

(*b*) The maximum value of the reverse flow occurs when the gap is about 1.5 times the channel width. When the gap is between 3 and 4 times the channel width the flow inside the channel is nearly stagnant. For higher gaps the flow in the inner channel is in the same direction as the outside flow, but even for a large gap the velocity is only about 65% of that outside.

(*c*) The magnitudes and the trend in variation of U_i/U_0 can be expected to remain nearly the same at Reynolds numbers equal to or above 4000.

Futher investigations are essential to fully understand this interesting flow phenomenon.

REFERENCES

ABERNATHY, F. H. & KRONAUER, R. E. 1962 The formation of vortex streets. *J. Fluid Mech.* **13**, 1–20.

BATCHELOR, G. K. 1967 *An Introduction to Fluid Dynamics*. Cambridge University Press.

CHANG, P. K. 1970 *Separation of Flow*, p. 345. Pergamon.

DAVIS, C. G. & SORENSON, K. E. (Eds) 1969 *Handbook of Applied Hydraulics*, pp. 37–29 to 37–37. McGraw-Hill.

EOM, K. 1988 Performance of a butterfly valve as a flow controller. *Trans. ASME* I: J. Fluids Engng **110**, 16–19.

GERRARD, J. H. 1966 The mechanics of the formation region of vortices behind bluff bodies. *J. Fluid Mech.* **25**, 401–413.

GERRARD, J. H. 1978 The wakes of cylindrical bluff bodies at low Reynolds numbers. *Phil. Trans. R. Soc. Lond.* A **288**, 351–382.

HUTCHISON, J. W. (Ed.). 1976 *ISA Handbook of Control Valves.*

KIYA, M. & MATSUMARA, M. 1988 Incoherent turbulence structure in the near wake of a normal plate. *J. Fluid Mech.* **190**, 343–356.

PERRY, A. E. & STEINER, T. R. 1987 Large-scale vortex structure in turbulent wakes behind bluff bodies. *J. Fluid Mech.* **174**, 233–270.

PIERCE, D. 1961 Photographic evidence of the formation and growth of vorticity behind plates accelerated from rest in still air. *J. Fluid Mech.* **11**, 460–464.

SMITS, A. J. 1982 A visual study of separation bubble. In *Proc. 2nd Intl. Symp. on Flow Visualisation, Bochum, Sept. 9–12, 1980* (ed. W. Merzkirch). Hemisphere.

STREETER, V. L. (Ed.) 1961 *Handbook of Fluid Dynamics*, pp. 21–29 to 21–40. McGraw-Hill.

TULAPURKARA, E. G., LAKSHMANA GOWDA, B. H. & BALACHANDRAN, N. 1988 Laminar flow through slots. *J. Fluid Mech.* **190**, 179–200.

UNAL, M. F. & ROCKWELL, D. 1988*a* On vortex formation from a cylinder. Part 1. The initial instability. *J. Fluid Mech.* **190**, 491–512.

UNAL, M. F. & ROCKWELL, D. 1988*b* On vortex formation from a cylinder. Part 2. Control by splitter-plate interference. *J. Fluid Mech.* **190**, 513–529.